JCI insight

IgV somatic mutation of human anti-SARS-CoV-2 monoclonal antibodies governs neutralization and breadth of reactivity

Mayara Garcia de Mattos Barbosa, … , Jeffrey L. Platt, Marilia Cascalho

JCI Insight. 2021. https://doi.org/10.1172/jci.insight.147386.

Research In-Press Preview COVID-19 Immunology

Graphical abstract

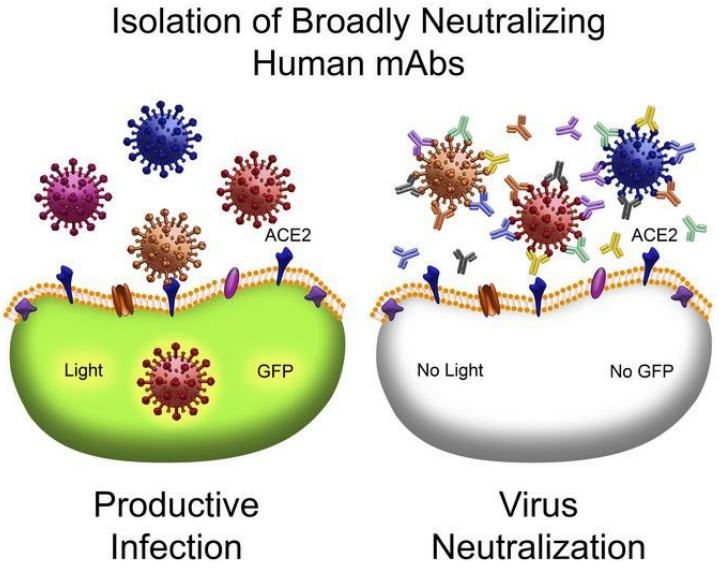

Title: IgV somatic mutation of human anti-SARS-CoV-2 monoclonal antibodies governs neutralization and breadth of reactivity

Authors: Mayara Garcia de Mattos Barbosa[1], Hui Liu[1], Daniel Huynh[1], Greg Shelley[2], Evan T. Keller[2,3], Brian T. Emmer[4,5], Emily Sherman[4,5], David Ginsburg[4,5,6], Andrew A. Kennedy[4], Andrew W. Tai[4], Christiane Wobus[7], Carmen Mirabeli[7], Thomas M. Lanigan[4,8], Milagros Samaniego[9], Wenzhao Meng[10], Aaron M. Rosenfeld[10], Eline T. Luning Prak[10], Jeffrey L. Platt[1,7,*], and Marilia Cascalho[1,7,*]

Affiliations:

[1]Department of Surgery, University of Michigan, Ann Arbor, MI, 48109, USA
[2]Department of Urology, University of Michigan, Ann Arbor, MI, 48109, USA
[3]Biointerfaces Institute, University of Michigan, Ann Arbor, MI, 48109, USA
[4]Department of Internal Medicine, University of Michigan, Ann Arbor, MI, 48109, USA
[5]Life Sciences Institute, University of Michigan, Ann Arbor, Michigan 48109, USA
[6]Departments of Human Genetics and Pediatrics and Howard Hughes Medical Institute, University of Michigan, Ann Arbor, MI, 48109, USA
[7]Department of Microbiology and Immunology, University of Michigan, Ann Arbor, MI, 48109, USA
[8]Vector Core, Biomedical Research Core Facilities, University of Michigan, Ann Arbor, MI 48109, USA
[9]Department of Medicine, Henry Ford Health Systems, Detroit, MI, 48202, USA
[10]Department of Pathology and Laboratory Medicine; Perelman School of Medicine; University of Pennsylvania; Philadelphia, PA, 19104, USA

*Correspondence: marilia@med.umich.edu (M.C.), plattjl@med.umich.edu (J.L.P.)

One Sentence Summary: Highly neutralizing SARS-CoV-2-specific human monoclonal antibodies isolated from memory B cells are broadly reactive and reactivity depends on V region somatic mutations.

The authors would like to dedicate this manuscript to Dr. Catarina Mota and her team, and to the staff at the Department of Medicine IIA at the "Hospital de Santa Maria" in Lisbon, Portugal, who valiantly fought and saved the lives of so many subjects with COVID under the most strenuous conditions.

Abstract:

Antibodies that neutralize SARS-CoV-2, are thought to provide the most immediate and effective treatment for those severely afflicted by this virus. Because coronavirus potentially diversifies by mutation, broadly neutralizing antibodies are especially sought. Here we report a novel approach to rapid generation of potent broadly neutralizing human anti-SARS-CoV-2 antibodies. We isolated SARS-CoV-2 Spike protein-specific memory B cells by panning from the blood of convalescent human subjects after infection with SARS-CoV-2, sequenced and expressed Ig genes from individual B cells as human monoclonal antibodies (mAbs). All of 43 human mAbs generated in this way neutralized SARS-CoV-2. Eighteen of the 43 human mAbs exhibited half-maximal inhibitory concentration (IC50s) of 6.7 $x10^{-12}$ M to 6.7$x10^{-15}$ M for spike pseudotyped virus. Seven of the human mAbs also neutralized with IC50<6.7 $x10^{-12}$ M viruses pseudotyped with mutant spike proteins (including receptor binding domain mutants and the S1 C-terminal D614G mutant). Neutralization of the Wuhan Hu-1 founder strain and of some variants decreased when coding sequences were reverted to germline, suggesting that potency of neutralization was acquired by somatic hypermutation and selection of B cells. The results indicate that infection with SARS-CoV-2 evokes high affinity B cell responses, some products of which are broadly neutralizing and others highly strain-specific. We also identify variants that would potentially resist immunity evoked by infection with the Wuhan Hu-1 founder strain or by vaccines developed with products of that strain, suggesting evolutionary courses SARS-CoV-2 could take.

Introduction

The immune response to SARS-CoV-2 is thought to promote clearance of the virus, recovery from clinical manifestations and protection against re-infection (1, 2). Among products of the immune response to SARS-CoV-2, antibodies capable of neutralizing SARS-CoV-2 are believed to be especially important for controlling severe manifestations of the disease (3). Administration of convalescent serum and monoclonal antibodies against the SARS-CoV-2 spike protein are reported to facilitate and hasten recovery from SARS-CoV-2 pneumonia (NCT04426695, NCT04425629, NCT04592549 and others) (4, 5). Yet unclear is whether any of individual antibodies or collection of antibodies thus far obtained effectively block variants of SARS-CoV-2 that have already emerged. Nor is it clear which among various approaches used to obtain anti-SARS-CoV-2 antibodies could rapidly adapt to control novel variants of this virus likely to emerge over time.

Immune serum and isolated immunoglobulins have been effective in multiple settings (6-9). However, availability from any given subject or pool of subjects is limited and not standardized. Furthermore, immune sera/plasma contain mixtures of antibodies, some of which might enhance the virus even though there is no evidence so far of enhancement in convalescent serum trials (10). These limitations motivate development of monoclonal antibodies (mAbs), especially human mAbs. Human mAbs are especially desired for at least three reasons. First, human mAbs can be generated directly from immune B cells without the time-consuming engineering needed to replace mouse with human sequences. Second, human mAb are less immunogenic than mouse monoclonal antibodies, even after "humanization," and hence less apt to generate immune complexes, extending their half-life. Third, human mAbs cloned from immune human B cells potentially reflect *in vivo* selection of cells expressing antibodies with anti-viral properties (11).

One challenge in developing human mAbs however is that the B cells most readily available are peripheral blood B cells and only a small fraction (usually less than 1%) of these are specific for any given antigen (12, 13). Accordingly, production of human mAbs generally requires the screening of numerous B cells, the preponderance producing antibodies that do not bind or only weakly bind the antigen of interest. We devised an approach that rapidly bypasses this problem and here report that isolating human mAbs from memory B cells that bind viral antigen under physiologic conditions yields a high percentage of neutralizing human mAbs.

Another hurdle to developing human mAbs anti-SARS-CoV-2 antibodies capable of controlling pathogenicity of the virus is genetic diversification and evolution of the virus. A number of SARS-CoV-2 variants have developed and spread in populations (14). Human antibodies directed against mutable viruses, like HIV, vary greatly in the diversity of strains recognized and effective control is associated with presence of broadly neutralizing antibodies in blood (15, 16). We tested the human mAbs we developed for neutralization of known SARS-CoV-2 strains and for ability to recognize SARS-CoV-2 spike protein variants that have developed across the world.

We describe here the approach we devised for rapid development of human monoclonal antibodies and show this approach can efficiently generate human neutralizing antibodies against prevailing strains of SARS-CoV-2. We also show the approach efficiently generates broadly neutralizing antibodies and that the characteristic of broad neutralization is associated with extensive mutation of Ig variable region sequences and likely with selection. As SARS-CoV-2 continues to evolve, effective control of severe disease might best be achieved by employing the strategies we describe to generate mixtures of highly-specific and broadly-reactive neutralizing antibodies.

Results

Plasma from convalescent patients neutralize pseudotyped viruses expressing reference and mutant strain spikes. To develop human monoclonal antibodies potentially capable of neutralizing multiple strains of SARS-CoV-2, we obtained B cells from human subjects who had experienced symptomatic infection with SARS-CoV-2 at least four weeks before and who had successfully cleared active virus. Although T cells and anti-SARS-CoV-2 Ab likely contributed to viral clearance, the interval of 4-8 weeks potentially allows somatic hypermutation (SMH) and selection to optimize the affinity of anti-SARS-CoV-2 Ab, increase the frequency of memory B cells circulating in blood and potentially minimizes the frequency of B cells producing enhancing Ab (10). Based on these criteria, we identified 12 convalescent volunteers (pertinent characteristics of the subjects are listed in the methods section) as sources of the B cells for generation of mAbs.

To verify the subjects had mounted protective antibody responses against SARS-CoV-2 and to compare monoclonal antibodies generated using B cells from those subjects, we devised a sensitive and stable assay for SARS-CoV-2

neutralization **(Figure S1)**. We modeled SARS-CoV-2 by introducing a SARS-CoV-2 spike protein on the surface of a third generation HIV lentivirus backbone to produce spike pseudotyped lentiviruses. To this end, a 19 AA C-terminal deletion of the S gene, encoding the spike protein from the Wuhan-Hu-1 or mutant SARS-CoV-2 strains, was transduced in human embryonic kidney (HEK) 293T/17 cells. The pseudotyped virus produced by the cells was used to assay neutralization. Spike pseudotyped lentiviruses infected 293T cells expressing angiotensin-converting enzyme 2 (ACE2), the SARS-CoV-2 receptor, in an ACE2-dependent manner and as efficiently as control VSV-G pseudotyped viruses **(Figures S1 and S2)**. In this assay, 4 out of the 12 convalescent plasmas had 50% neutralization titers (ID50) above 1/100, indicating a fraction of the subjects had appreciable neutralizing responses to SARS-CoV-2 infection.

Isolation of memory B cells with high avidity for SARS-CoV-2 Spike protein. Human mAbs against SARS-CoV-2 have been generated by single-cell cloning of Ig genes from peripheral blood B cells (3, 4, 17-21). One surprising finding was that anti-SARS-CoV-2 neutralizing antibodies were not heavily mutated. We reasoned we could optimize the development of biologically active human antibodies with high neutralizing potency by using as the source of DNA memory B cells with antigen receptors that avidly bind antigen of interest under physiologic conditions. Accordingly, peripheral blood mononuclear cells were incubated for 72 hours in medium containing CpG, CD40L, IL-2, IL-15 and IL-21, which favor survival and expansion of memory B cells (22). The cultured cells were then transferred to wells containing SARS-CoV-2 S1 antigen in native configuration, incubated for 24 hours followed by isolation of antigen-specific B cells by panning at 37^{o}C (11, 20, 23). Panned cells were then cultured with the cytokine cocktail for an additional 48 hours. The specificity of the B cells was confirmed by ELISPOT **(Figure S3)**.

In samples from six recovered subjects, the frequency of IgG-producing spike-specific B cells as a fraction of the total IgG-producing cells increased with the neutralization titer of the plasma. Thus, following 6 days of culture 8%, 2% and 13.3% (of subjects #2, #3 and #4 respectively) of IgG+ memory B cells secreted antibodies that bound to the spike protein. In contrast, healthy controls or previously infected patients with low plasma neutralization titer had few or no spike-specific B cells.

Spike-specific B cells encode mutated antibodies. We performed single-cell sequencing of spike-specific B cells, obtained from 11 subjects followed by paired end single index Ig sequencing. Clonally related B cells were defined as

having the same IGHV gene, IGHJ gene, CDR3 length and 85% identity in the CDR3 amino acid sequence, as described previously (24, 25). We obtained more than 6,000 spike-specific Ig clones. The frequency of IgM clones varied from a minimum of 35.7% to a maximum of 84.3%, the frequency of IgG isotypes varied between 8.0% and 53.7% and the frequency of IgA isotypes varied between 1.4% and 15.1%. **(Figure 1A)**. Average IgA usage was almost two-fold higher in subjects with higher plasma neutralization titers (ID50>1/50; 9.1%) compared subjects with plasma neutralization titers lower than 1/50 (5.5%) **(Figure 1A)**. In contrast, the frequencies of IgM and IgG1-encoding isotypes did not differ significantly between individuals with higher *vs.* lower neutralization titers.

To determine the frequency of spike-binding Ig clones in the blood, paired-end bulk sequencing was performed on the same donors, as described in the methods section. Spike-specific Ig clones were relatively rare in the blood (< than 0.1% of all B cell clones) **(Figure 1B)**. Some VH3 family members appeared to be enriched (>2-fold) in the spike-specific libraries (IGHV 3-30, IGHV 3-13, IGHV 3-23, IGHV 3-72, IGHV 3-73 and IGHV 3-66), **(Figures 2A and 2B)**. Other studies (26), found that 10% of SARS-CoV-2 neutralizing antibodies were encoded by IGHV 3-53, at a frequency at least 4 times higher than that observed in the blood of naïve healthy individuals (29,30). These antibodies had few somatic mutations, and Yuan et al. (26) found that recognition ACE2 by the RBD was mediated by germline encoded residues (NY motif at VH residues 32 and 33 in the CDRH1 and an SGGS motif at VH residues 53 to 56 in CDRH2) suggesting that neutralization potency was dissociated from affinity maturation. In contrast, our single-cell data suggests that strongly neutralizing antibodies are somatically mutated **(Figures 3A and 3B)**. In particular, the frequency IgG or IgA clones that harbored VH sequences with SMH increased with serum neutralization titers. For sequences with >10% SHM, contingency analysis between weak and strongly neutralizing groups by Chi-square test yielded p=0.0066 for IgG and p=0.0022 for IgA. We also found that only one out of 274 IgA clones obtained from subjects with high neutralizing serum (ID50>1/200) was un-mutated while 44 of 214 (20.6%) IgA clones obtained from subjects with low neutralizing serum (ID50<1/50) were germline and had, on average, 2 AA smaller CDR3 regions. These findings suggested that adaptive IgA/IgG responses contribute to neutralization.

Generation of SARS-CoV-2 highly neutralizing antibodies. To generate human mAbs specific for SARS-CoV-2 spike, we cloned the IgH and IgL variable regions 3' to the human IgG1 constant region (27, 28). We selected IgV sequences of IgG or IgA antibodies, with mutated V_H regions (> 5% compared to their closest germline) and that were represented in the

sequencing pool by multiple copies. We expressed Ig VH and VL pairs generating 43 recombinant spike-specific antibodies from SARS-CoV-2-specific B cells. (27, 28). Antibody concentrations were determined by ELISA and neutralization potency determined against pseudotyped viruses, as indicated on **Figure S1**. All 43 monoclonal antibodies synthesized neutralized Wuhan-Hu-1 spike pseudotyped virions, 18 of 43 antibodies neutralized spike pseudotyped viruses with extremely high potency, with half-maximal inhibitory concentration (IC50) < 1ng/mL (6.7×10^{-12} M). Four of the mAbs (#22, #13, #21 and #27) had IC50s close to 1 pg/mL (6.7×10^{-15} M) **(Figures 4A and 4B)**. These IC50s are comparable to the most powerful antibodies produced by Regeneron (4) and by others (3, 21, 23, 29)and tested by a pseudotyped virus assay similar to ours. Monoclonal antibody #19 did also neutralize live WA1 virus with comparable IC50s **(Figure 4C),** indicating, as others have shown (17), that IC50s determined by pseudotyped virus assay closely reflect neutralization potencies against live viruses. Neutralization potency increased with the number of mutations in the VH and VL exons of the 11 mAbs with the lowest IC50s **(Figure 4D)** suggesting that affinity maturation contributes to high neutralization potency. To directly test the contribution of SMH to neutralization potency we reverted VH and VL sequences of mAbs #5, #13, #15 and #20 to their germline configuration and tested their neutralization potency. **Figure 4E** shows that germline encoded antibodies neutralized pseudotyped viruses expressing the Wuhan-Hu-1 spike much less efficiently, by at least 1000-fold, than their mutated counterparts indicating that SHM contributed to increased neutralization efficiency in these antibodies.

SARS-CoV-2 highly neutralizing antibodies are broadly reactive. To determine if natural infection induced broadly neutralizing antibodies, we tested neutralization of pseudotyped viruses with spike protein variants in the S1 N-terminal domain (H49Y, V247R, V367F, R408I), in the receptor-binding domain (V483A, H519Q, A520S) and in the S1-C-terminal domain (D614G). Of these variants A520S and D614G have notably greater infectivity than wild type Wuhan-Hu-1(30). Testing of plasma revealed notable variation in specificity for variants. While plasma #3 exhibited broad neutralization, plasma from subject #102 did not neutralize at all Wuhan-1, D614G, S247R and H49Y spike pseudotyped viruses but neutralized moderately H519Q, and A520S spike pseudotyped viruses suggesting that the plasma contains antibodies with narrow specificity for the mutant RBD **(Figures S4A and S4B)**. In another notable result plasma from subject #4 neutralized H519Q spike pseudotyped viruses 100-fold more potently than any other spike pseudotyped viruses. (Figures S4A and S4B). However, serology alone could not determine whether these differences reflected differences in breadth of neutralization of individual antibodies or merely the diversity of antibodies present in the plasma.

To distinguish between these two possibilities, we next tested the ability of mAbs with the highest potency (IC50<6.7 x 10^{-12} M; mAbs #1, #2, #5, #13, #15 and #20) for breadth of neutralization of variants. Most mAbs with high potency against Wuhan-Hu-1 spike pseudotyped virus also neutralized variants of that strain but with 10 to 100-fold less potency **(Figure 5A)**. The most powerful mAbs were the least cross-reactive. For example, mAb# 13 neutralized virus with Wuhan-Hu-1 spike at IC50 of 8.3 x 10^{-14} M, but exhibited ~100-fold less neutralizing potency against the mutants tested **(Figures 5A-C)**. As another example, mAb# 15 neutralized Wuhan-Hu-1 at IC50 of 3.0 x 10^{-13} M but had 10 to 100-fold lower potency against most mutants. Monoclonal Ab #5, #1 and #2 were notably potent against Wuhan-Hu-1 (IC50 varying from 7.4 x 10^{-13} for mAb #5 to 4.1 x 10^{-12} M and 4.3 x 10^{-12} M, for mAbs #1 and #2, respectively) also had 10 to 100-fold lower potency against most mutants. However, mAb #20 neutralized Wuhan-Hu-1 at IC50 of 5.3x 10^{-10} M but neutralized D614G mutants with higher potency at IC50 of 3.5 x 10^{-10} M **(Figures 5A-C)**. Neutralization of D614G mutants by mAb #20 (and also by mAbs #5, #13 and #15) depended on somatic mutations since the germline-encoded antibody was at least 100-fold less efficacious **(Figure 6)**. Interestingly, germline mAbs #20, #13 and #15 neutralized H49Y spike mutants as well their mutated counterparts **(Figure 6)** indicating that the H49Y mutation does not perturb the binding epitope responsible for neutralization. Neutralization of A520S spike mutants by mAbs #5, #13 and #15 but not by mAb #20 depended on somatic mutations **(Figure 6)**. Data indicate that SMH of antibodies is necessary for high potency neutralization but that some broad-reactivity may be explained by properties afforded by the germline precursors of the mature mutated antibodies.

Discussion

We adapted an approach, originally developed to isolate donor-specific B cells from blood of transplant recipients, to the rapid and efficient generation human monoclonal antibodies with high and broadly neutralizing potency against SARS-CoV-2. Our approach includes a brief incubation of PBMCs with a cytokine cocktail and exposure to antigen in native form in cell culture to selectively recover memory B cells specific for the antigen of interest (22). Using avidity binding to immobilized native antigen as an initial step, we avoided time-consuming screening of unselected B cells, and are able to focus rapidly on selecting B cells with optimized specificities. In this way, we generated highly neutralizing mAbs without any further screening, in less than 6 weeks. All 43 antibodies that we produced had high neutralization capability against SARS-CoV-2 viruses. Although the antibodies generated in this way have not been tested for clinical efficacy, the potency of neutralization exceeds by orders of magnitude the potency

of neutralization of human mAbs currently in clinical trials (NCT04426695, NCT04425629, NCT04592549 and others) (4, 5).

Even more important may be the ability of these antibodies to neutralize mutant strains. It is clear that diversification of SARS-CoV-2 has already occurred in populations. The CoV-GLUE database (14) reports >5,300 distinct non-synonymous mutations in the gene encoding the spike in natural SARS-CoV-2 populations. The significance of many variants for infectivity, spreading and immune evasion is at present unknown but recent research suggest that some mutations may increase severity of disease and/or virus infectivity. Becerra-Flores et al. (31) suggested a causal link between D614G variants and increased fatality in COVID-19 patients. Qianqian Li et al. (30) found that the D614G and the RBD A520S spike variant increased infectivity of pseudotyped viruses. Most recently, Hou et al. (32) found that the D614G mutation increased virus infectivity, competitive fitness and transmission in primary human cells and in animal models.

Although we do not yet know if immunity drives virus evolution evidence supports this possibility. Variants that are resistant to neutralizing antibodies have increased in frequency since the beginning of the pandemic (33, 34). Baum et al. (4) and Weisblum et al. (33) report that neutralizing antibodies readily select for resistant virus after *in vitro* passaging, even though coronavirus immune escape is not yet known to influence pathogenicity in individual patients. In theory, broadly neutralizing antibodies are less forgiving of diversification and hence variants in a population could be less likely to emerge when broadly neutralizing Abs are present. Although not the main objective of our work and even if variants may arise owing to increasing virus fitness, the results presented here offer a glimpse at viral variants that might evade typical Ab responses and hence increase in frequency as SARS-CoV-2 evolves. Our results indicate that D614G and A520S variants are more resistant to neutralizing antibodies than viruses with the Wuhan Hu-1 spike suggesting that immunity elicited against the Wuhan Hu-1 (the prevalent strain in Michigan at the time of sample collection) might fuel escape variants. It is noteworthy that some of the described public antibodies to SARS-CoV-2 have minimal levels of SHM (35). This finding, similar to what has been described for other newly encountered pathogens (36), suggest that the naïve repertoire contains antibodies that can bind and neutralize the virus. Consistent with this, antibodies (like mAb #20) have modest IC50s and exhibit cross reactivity against SARS-CoV-2 with A520S and H49Y spike mutations. This cross-reactivity is retained, even when mAbs are reverted to their germline sequences. This result suggests that some cross-reactivity may depend on properties of germline-encoded antibodies. However, as the virus evolves, such “germline-encoded” antibodies may become less effective. Monoclonal Abs with high neutralization potency (#5, #12, #13 and #15) neutralized variants much

less effectively than the original strain. Furthermore, reverting VH+VL sequences of those antibodies to their germline configuration decreased neutralization potency against the reference strain but also against variant strains suggesting that mutations helped with the establishment of cross-reactivity.

As a contrasting example, a virus that has accumulated higher levels of mutation, such as HIV, poses a far more challenging target to the immune system. Broadly neutralizing antibodies to HIV are very infrequent in the primary repertoire and often harbor unusual sequence features (such as long CDR3s) and are typically highly mutated. Indeed, the canonical broadly neutralizing Abs to HIV, when reverted to their germline sequences, have significantly diminished neutralizing ability (37, 38). Our results indicate that, SARS-CoV-2 infection induces mutated antibodies (#2, #5, #12, #13 and #15), albeit less so than broadly neutralizing antibodies evoked by long lasting HIV infection, that retain broadly neutralizing capacity although at a reduced potency compared to the infecting strain neutralization potency. Very high affinity antibodies that can broadly neutralize multiple virus variants are desirable as potential therapeutics because they would decrease the necessity of testing and producing monoclonal antibody cocktails to neutralize many different virus variants.

Our results also reveal some properties of the virus-specific Ig clones that are highly relevant to immune memory. A subset of the spike-specific Ig clones encoded by IgG and IgA isotypes have properties we would expect to encounter in Ig genes of B cells engaged in active T-dependent antibody responses. Somatic mutations in IGHV genes of spike-specific IgG and IgA B cells increased with plasma neutralization titers. Thus, the frequency IgG or IgA clones with IGHV genes that exhibited 10% or higher levels of SHM increased with plasma neutralization titers. Furthermore, the neutralization potency of the 11 most powerful MAbs increased directly with the number of somatic mutations in the IGHV and IGLV genes. Our findings contrast with Yuan et al. (26) who compiled a list of 294 anti-SARS-CoV-2 RBD targeting antibodies identified by 12 different groups and found that 10% were encoded by IGHV 3-53 and had few somatic mutations. These authors also found that recognition of the ACE2 binding site was mediated by germline-encoded residues suggesting that neutralization potency is dissociated from affinity maturation. It is possible that differences in the properties of antibodies found by different groups and by us is due to the time of analysis relative to the beginning of disease and/or disease severity (39). It is also possible that the public SARS-CoV-2-reactive antibodies that have been described to date are biased towards those that have low levels of SHM because such antibodies are easier to identify than mutated antibodies with sequence variations. Furthermore, how generalizable our knowledge of public SARS-CoV-2 clones is to defining the overall immune

response to SARS-CoV-2 is not yet clear as we and others have shown that the vast majority of SARS-CoV-2-binding antibodies are private (35, 40).

The antibodies here reported were obtained from subjects 4 to 8 weeks from beginning of disease and who had disease severe enough to require hospitalization. Consistent with this view, Gaebler et al. (13) have recently found that antibody maturation persists during recovery. In their study, the number of mutations in VH and VL sequences increased in every one of the 6 individuals followed up to 6 months after their initial diagnosis even though their serum neutralizing titers decreased over the same time interval, suggesting that the maturation of virus-specific antibodies occurred in memory B cells. Studying the properties and ability of memory B cell responses to accommodate sequence variations in SARS-CoV-2 is important for our understanding of the durability of protective immunity in vaccinated and infected individuals.

Methods:

Experimental Subjects

Human subjects were recruited from Covid-19 convalescent patients followed at the University of Michigan Hospital or at the Henry Ford Health System. We have enrolled 12 convalescent patients recovering from COVID-19 infection. Eight patients were from Michigan Medicine and 4 were from Henry Ford Health System. Subjects were between 29 and 73 years old and were free of virus (and symptoms) at the time of enrollment. Most had co-morbidities such as diabetes, obesity and/or heart disease. Six had been seriously ill, requiring intensive care, five had been hospitalized but had not required intensive care, one was not hospitalized and recovered at home. All blood samples were collected at least 4 weeks and less than 8 weeks after the beginning of symptoms and patients were virus-free at blood collection. Heparinized blood samples were obtained, the plasma was collected and heat-inactivated at 56°C for 1 hour. The original sample volume was restored by adding PBS and the peripheral blood mononuclear cells (PBMCs) were isolated with Ficoll-Paque PLUS density gradient media (Cytiva, Cat#17-1440-02). Samples were frozen and stored in a nitrogen tank until posterior use.

The 293T-ACE2 cell line

To ensure optimal transduction we produced a 293T cell line that overexpresses the SARS-CoV-2 receptor the angiotensin-converting enzyme 2 (ACE2), the 293T-ACE2 cells. Lentivirus packaging vectors psPAX2 (3.5 µg, Addgene, Cat#12260, RRID: Addgene_12260), and pC1-VSVG (3.5 µg, Addgene, Cat#1733, RRID: Addgene_1733) were co-transfected with 7 µg of pLenti-ACE2 proviral plasmid using standard polyethyleneimine (PEI) precipitation methods. Polyethyleneimine precipitation was performed by incubating the plasmids with 42 µg PEI molecular weight 25,000 (Polysciences, Inc, Cat#23966-1) in 1 mL Opti-MEM I Reduced Serum Medium (Gibco, cat#31985070) at room temperature for 20 minutes, before adding it to 8 mL of DMEM, high glucose media (Life Technologies, Cat#11965092) supplemented with 10% heat-inactivated Fetal Bovine Serum (FBS) 1X Glutamax (Gibco, cat#35050-061) 100 U/mL Pen Strep (Gibco, Cat#15140-122). This DNA/PEI-containing media was then distributed to a T-75 flask containing 293T/17 [HEK 293T/17] cells (ATCC, CRL-11268, RRID: CVCL_1926). The lysate was collected after 72 hours, spun at 2000 *rpm* in a Beckman 5810R tabletop centrifuge for 10 minutes to pellet any cell debris. The supernatant containing Lenti-ACE2-VSV-G was then stored in aliquots at -80°C. A 6-well plate of 293T/17 cells was created 24 hours prior to transduction, to attain 50% of confluence on the day it was transduced. The plate was then transduced with 1.5 mL per well of 1X Lenti-ACE2-VSV-G lentivirus

supernatant on 5 wells, and the final well was maintained as a negative control, containing only DMEM 10% FBS 1X Glutamax 100 U/mL Pen Strep. Twenty-four hours post-transduction, the media was changed on all 6 wells, and after 48 hours of transduction, the media was supplemented with 3µg/mL puromycin dihidrochloride (Gibco, Cat#A1113803). The cells were cultured under selective pressure for 6 days, until the cells on the control well were completely dead. The selected cells were harvested and amplified under puromycin selection (1µg/mL).

Lenti-GF1 SARS-CoV-2 Wuhan-Hu-1 and mutated spike pseudotyped viruses

Lentivirus packaging vectors psPAX2 (3.5 µg, Addgene, Cat#12260, RRID: Addgene_12260), and SARS-CoV-2 truncated spike envelope pSARS-CoV-2Δ19AA (35 µg) were co-transfected with 70 µg of pGreenFire1(GF1)-CMV pro-viral plasmid (System Biosciences, cat#TR011VA-1) using standard PEI precipitation methods. The plasmid expresses both GFP and luciferase allowing interchangeable detection of virus infected cells by fluorescence and luminescence readouts. Polyethyleneimine precipitation was performed by incubating the plasmids with 420 µg PEI in 10 mL Opti-MEM I Reduced Serum Medium at room temperature for 20 minutes, before adding to 90 mL DMEM 10% FBS 1X Glutamax 100 U/mL Pen Strep. The DNA/PEI-containing media was then distributed equally to 5-T150 flasks containing 293T/17 cells. Supernatants were collected and pooled after 72 hours, filtered on a 0.45-micron GP Express filter flask (Millipore), pelleted by centrifugation at 13,000 *rpm* on a Beckman Avanti J-E centrifuge at 4°C for 4 hours, and resuspended at 100X the original concentration (~1×10^7 TU/ml) in DMEM. The lentivirus was stored in aliquots at -80°C. Alternatively, Lentivirus Lenti-GF1-SARS-CoV-2Δ19AA truncated spike envelope displaying the H49Y, S247R, V367F, R408I, V483A, H519Q, A520S and D614G mutations were produced using the same method. Variants were selected based on their prevalence in the wild, evidence of high infectivity or increased fitness, and chosen to target the verious domains of the spike protein including the receptor binding domain (H519Q, A520S).

Neutralization assays

293T/17, 293T-ACE2, and VeroE6 (VERO C1008, ATCC, Cat# CRL-1586, RRID: CVCL_0574) cell lines were platted 24 hours prior to transduction to obtain 50% confluence on the day of transduction. To test efficiency of Spike-pseudotyped virus transduction, concentrated virus or supernatant was added to cells in varying amounts. For neutralization assays 293T-ACE2 were used. Heat-inactivated plasma or monoclonal antibodies samples were serially diluted into DMEM 10% FBS 1X Glutamax 100 U/mL Pen Strep. Plasma or antibody dilutions were then incubated with ~2.66 x 10^5 TU/mL Lenti-GF1

virus pseudotyped with Wuhan-Hu-1 SARS-CoV-2Δ19AA or mutant spikes for 30 minutes at room temperature prior to transduction. After neutralization, cells were transduced with the virus-plasma/antibody solution, virus-10 μg/mL human IgG (Southern Biotech, Cat# 0150-01) or virus alone and incubated at 37°C 5% CO_2. Luminescence and GFP expression were analyzed 72 hours post-transduction by luciferase assay, flow cytometry and/or fluorescence microscopy. Assays were repeated at least 3 times and IC50 calculates from curves spanning 0% to 100% neutralization.

Luciferase assay

Chemiluminescence was detected using the Bright-Glo Luciferase Assay System (Promega, #E2620) according to the manufacturer instructions. Briefly, the excess supernatant from the transduced plates was discarded leaving 50 μL of cell culture media, 50 μL of the Bright-Glo reagent equilibrated at room temperature was then added and the cells were incubated for 5 minutes to allow complete cell lysis. After incubation the cell lysates were transferred to 96-well white plates and read on a Synergy 2 plate reader (Biotek Instruments, Winooski, VT).

Spike-specific B cell panning and single cell V(D)J analysis

Covid-19 convalescent patients PBMCs were thawed, 1 x 10^6 cells per mL of media were cultured in RPMI 1640 (Gibco, Cat#11875093) supplemented with L-Glutamine 10% FBS 100 U/mL Pen Strep 0.1% 2-mercapthoethanol 5μM CpG ODN 2006 10 ng/mL CD40L 50 ng/mL IL-2, 2 ng/mL IL-15 10 ng/mL IL-21 (cytokine cocktail media) (22) for 72 hours at 37ºC 5% CO_2 and cells were retrieved, resuspended at 1 x 10^6 cells per mL in fresh cytokine cocktail media and then transferred to wells coated with rabbit anti-Avi-tag antibody (4 μg/mL, GenScript, Cat#A00674, RRID: AB_915553) bound to S1-C-6HIS-Avi (4 μg/mL, ABclonal, Cat#RP01261) previously blocked with PBS 10% FBS. After a 24-hour incubation at 37°C 5% CO_2, the plates were washed twice with RPMI 1640 supplemented with L-Glutamine 10% FBS 100 U/mL Pen Strep 0.1% 2-mercapthoethanol at 37°C to remove non-bound cells. The cytokine cocktail media was then replenished and the plates were cultured at 37ºC 5% CO_2 for additional 48 hours. Bound cells were harvested by vigorous pipetting and up to 10,000 cells were analyzed by Chromium Next Gel Bead-in-Emulsions (GEM) Single Cell V(D)J Technology. Briefly, cells were identified via generation of GEMs by combining barcoded Single Cell V(D)J 5' Gel Beads v1.1, a master mix with cells (Chromium Next GEM Single Cell 5′ Library and Gel Bead Kit v1.1; 10x Genomics, Cat#1000165), and partitioning Oil on Chromium Next GEM Chip G (Chromium Next GEM Chip G Single Cell Kit; 10x Genomics, Cat#1000120) and reverse transcription and cDNA amplification were performed as recommended by the manufacturer.

Next, the targeted enrichment from cDNA was conducted with the Chromium Single Cell V(D)J Enrichment Kit, Human B Cell (10x Genomics, Cat#1000016). The cDNA quality control (QC) analysis was carried out in an Agilent 2100 Bioanalyzer (Agilent Technologies, Santa Clara, CA) using the Agilent High Sensitivity DNA Kit (Agilent Technologies, Cat#5067-4626). The V(D)J enriched library was then constructed via Chromium Single Cell 5' Library Construction Kit v1.1 (10x Genomics, Cat#1000166) and libraries were sequenced in a NovaSeq™ 6000 Sequencing System (Illumina, San Diego, CA). Chromium single-cell RNA-seq output was processed in the Cell Ranger pipelines (10x Genomics, Pleasanton, CA, RRID:SCR_017344) and the V usage and clonotype profiles were generated and visualized by Loupe VDJ Browser.

Bulk sequencing of IgH rearrangements from PBMCs

IgH gene rearrangements were amplified from genomic DNA obtained from PBMCs and sequenced with an Illumina MiSeq as previously described in (24). For each subject, two biologically independent libraries each containing 100 ng input gDNA were generated and sequenced. For two of the subjects (1 & 101), spike-specific samples were additionally sequenced also each with two replicates.

Analysis of bulk IGHV gene rearrangements from PBMC gDNA

Sequences were paired and quality controlled with pRESTO (24), as described in (41) and annotated with IgBLAST (42) using default parameters and the IMGT reference database (43). The resulting data were imported into ImmuneDB (44) for further downstream analyses.

Ig Heavy and Light chains cloning and expression.

IgG heavy and light chain variable regions were cloned into human Igγ1, Igκ and Igλ expression vectors (pFUSE2ss-CLIg-hK; Invivogen, Cat#pfuse2ss-hclk) containing multiple cloning site upstream of the human γ constant region (45). Eblock fragments for the variable regions were generated by IDT and had arms attached to allow for Gibson assembly. Eblock fragments were then inserted into their respective expression vector using Gibson assembly (New England Biolabs) following the manufacturer's instructions and transformed into NEB Stable Competent *E. Coli* (New England Biolabs, Cat# C3040I). Plasmid DNA was isolated from 2 mL cultures, mini prepped using a Qiagen QIAprep Spin Miniprep Kit (QIAGEN, Cat# 27106). Sequence of insert was confirmed by Sanger sequencing from Eurofins using the following sequencing primer (pMT2-F 5'-TTGCCTTTCTCTCCACAGGT-3'). Heavy and light chain plasmids were co-transfected

into 293T/17 cells using standard PEI precipitation methods. Polyethyleneimine precipitation was performed to obtain 9 mL of mAbs, incubating 7 µg of both light and heavy chain plasmids with 42 µg PEI molecular weight 25,000 (Polysciences, Inc, Cat#23966-1) in 1 mL Opti-MEM I Reduced Serum Medium at room temperature for 20 minutes, before adding it to 9 mL of DMEM, high glucose 10% FBS 1X Glutamax 100 U/mL Pen Strep. This DNA/PEI-containing media was then distributed to a T-75 flask containing 293T/17 cells. The supernatant was collected after 72 hours, spun at 2000 *rpm* in a Beckman 5810R tabletop centrifuge for 10 minutes to pellet any cell debris and transferred to a fresh tube. Alternatively, to obtain 60 mL of mAbs supernatant, 42 µg of light and heavy chain DNA were co-transfected after precipitation with 252 ug PEI in 1 mL Opti-MEM I Reduced Serum Medium, before adding to 60 mL of DMEM, high glucose 10% FBS 1X Glutamax 100 U/mL Pen Strep, distributed to 2 T-225 flasks containing 293T/17 cells.

50% Tissue Culture Infectious Dose Assay. For the TCID50 assay, 96-well plates were seeded with VeroE6 (VERO C1008, ATCC, Cat# CRL-1586, RRID: CVCL_0574) at 20,000 cells per well for near confluence at 37°C for 24 hours. Plates and 460 µL of antibody dilutions were transferred to BSL3 facility and antibody solutions were incubated with 40 µL of live SARS-CoV-2 USA-WA1/2020 clinical isolate viral solution for an MOI of 0.1. Antibody and virus solutions were incubated at 37°C for 1 hour. 100 µL of the viral solutions were diluted in 900 µL 2% FBS DMEM for -1 dilutions and 10 µL of solution were added to 8 replicate wells of a 96-well plate for a -2 dilution. From the -2 dilutions, serial dilutions were performed for a range of -2 to -7 for experimental conditions, and -4 to -7 for untreated infection controls. Plates were incubated at 37°C for 3 days, then examined microscopically for visible cytopathic effect (CPE). Viral titer was then calculated from number of CPE-positive wells using a modified Reed and Muench method.

Statistics. All comparisons were done with GraphPad Prism 8 software (GraphPad Software, La Jolla, CA, RRID:SCR_002798). Averages were compared by paired, unpaired t test, nonparametric Mann-Whitney test or Wilcoxon test for paired analysis. A P value of equal or less than 0.05 was considered significant. Non-linear fit analysis of neutralization curves was used to determine IC50 and ID50 values using the GraphPad Prism "Absolute IC50, X is log (concentration)" option.

Study Approval

Human subjects were recruited from Covid-19 convalescent patients followed at the University of Michigan Hospital or at the Henry Ford Health System. All human subjects consented to these studies and research was approved by the Institutional Review Boards at the University of Michigan and at the Henry Ford Health System.

Author Contributions

MC and JLP designed the research. MC, JLP and MGMB analyzed results and wrote the manuscript. MGMB, HL, DH, GS, BTE, ES, AAK, CM, TML, WM and AMR performed experiments and helped in the analysis of results. TML, DG, AWT, CW, and ETLP planned or analyzed specific experiments including those with live virus (AWT, CW), sequencing and analysis of Ig sequences (ETLP). MS assisted with collection of patient samples and the evaluation of their clinical history. DG and ETK participated in the discussion and writing of the manuscript.

Acknowledgements

The research was supported by the NIH (R01 AI51588 01, R01 AI122369 to M.C., P01 CA093900 to E.T.K.), by a University of Michigan Cardio Vascular Center Impact Research Ignitor Grant Award (to M.C.), Biointerfaces Institute Award for COVID research (ETK and MC), a MICHR Accelerating Synergy Award (to M.C.) and and MICHR Education PTSP 2020 (U069943 to M.G.M.B.) and by a grant of the National Cancer Institute of the National Institutes of Health under Award Number P30CA046592 by the use of the following Cancer Center Shared Resource: Single Cell Analysis Shared Resource. We would like to acknowledge the enthusiasm and support of Dr. David Pinsky that was crucial to get the research started. We would also like to thank members of the clinical team who helped us collect samples from subjects recovering from COVID-19 in particular Nicholas L. Harris of the Clinical Trials Support Unit at the University of Michigan and Dr. Iman Bajjoka, Pharm.D., BCPS, FCCP, Director, Transplant Operational Research at the Henry Ford Transplant Institute.

References:

1. Grifoni A, Weiskopf D, Ramirez SI, Mateus J, Dan JM, Moderbacher CR, et al. Targets of T Cell Responses to SARS-CoV-2 Coronavirus in Humans with COVID-19 Disease and Unexposed Individuals. *Cell.* 2020;181(7):1489-501 e15.
2. Ni L, Ye F, Cheng ML, Feng Y, Deng YQ, Zhao H, et al. Detection of SARS-CoV-2-Specific Humoral and Cellular Immunity in COVID-19 Convalescent Individuals. *Immunity.* 2020;52(6):971-7 e3.
3. Zost SJ, Gilchuk P, Case JB, Binshtein E, Chen RE, Nkolola JP, et al. Potently neutralizing and protective human antibodies against SARS-CoV-2. *Nature.* 2020;584(7821):443-9.
4. Baum A, Fulton BO, Wloga E, Copin R, Pascal KE, Russo V, et al. Antibody cocktail to SARS-CoV-2 spike protein prevents rapid mutational escape seen with individual antibodies. *Science.* 2020;369(6506):1014-8.
5. Tu YF, Chien CS, Yarmishyn AA, Lin YY, Luo YH, Lin YT, et al. A Review of SARS-CoV-2 and the Ongoing Clinical Trials. *Int J Mol Sci.* 2020;21(7).
6. Abolghasemi H, Eshghi P, Cheraghali AM, Imani Fooladi AA, Bolouki Moghaddam F, Imanizadeh S, et al. Clinical efficacy of convalescent plasma for treatment of COVID-19 infections: Results of a multicenter clinical study. *Transfus Apher Sci.* 2020:102875.

7. Einollahi B, Cegolon L, Abolghasemi H, Imanizadeh S, Bahramifar A, Zhao S, et al. A patient affected by critical COVID-19 pneumonia, successfully treated with convalescent plasma. *Transfus Apher Sci.* 2020:102995.
8. Shen C, Wang Z, Zhao F, Yang Y, Li J, Yuan J, et al. Treatment of 5 Critically Ill Patients With COVID-19 With Convalescent Plasma. *JAMA.* 2020;323(16):1582-9.
9. Zheng K, Liao G, Lalu MM, Tinmouth A, Fergusson DA, and Allan DS. A Scoping Review of Registered Clinical Trials of Convalescent Plasma for COVID-19 and a Framework for Accelerated Synthesis of Trial Evidence (FAST Evidence). *Transfus Med Rev.* 2020;34(3):158-64.
10. Casadevall A, and Pirofski LA. The convalescent sera option for containing COVID-19. *J Clin Invest.* 2020;130(4):1545-8.
11. Barnes CO, West AP, Jr., Huey-Tubman KE, Hoffmann MAG, Sharaf NG, Hoffman PR, et al. Structures of Human Antibodies Bound to SARS-CoV-2 Spike Reveal Common Epitopes and Recurrent Features of Antibodies. *Cell.* 2020;182(4):828-42 e16.
12. Mouquet H, Klein F, Scheid JF, Warncke M, Pietzsch J, Oliveira TY, et al. Memory B cell antibodies to HIV-1 gp140 cloned from individuals infected with clade A and B viruses. *PloS one.* 2011;6(9):e24078.
13. Gaebler C, Wang Z, Lorenzi JCC, Muecksch F, Finkin S, Tokuyama M, et al. Evolution of Antibody Immunity to SARS-CoV-2. *bioRxiv.* 2020.
14. Joshua B Singer RJG, Matthew Cotten and David L Robertson. CoV-GLUE: A Web Application for Tracking SARS-CoV-2 Genomic Variation. *PrePrints.* 2020:2020060225.
15. Scheid JF, Mouquet H, Feldhahn N, Seaman MS, Velinzon K, Pietzsch J, et al. Broad diversity of neutralizing antibodies isolated from memory B cells in HIV-infected individuals. *Nature.* 2009;458(7238):636-40.
16. Zolla-Pazner S. Identifying epitopes of HIV-1 that induce protective antibodies. *Nat Rev Immunol.* 2004;4(3):199-210.
17. Robbiani DF, Gaebler C, Muecksch F, Lorenzi JCC, Wang Z, Cho A, et al. Convergent antibody responses to SARS-CoV-2 in convalescent individuals. *Nature.* 2020;584(7821):437-42.
18. Pinto D, Park YJ, Beltramello M, Walls AC, Tortorici MA, Bianchi S, et al. Cross-neutralization of SARS-CoV-2 by a human monoclonal SARS-CoV antibody. *Nature.* 2020.
19. Rogers TF, Zhao F, Huang D, Beutler N, Burns A, He WT, et al. Isolation of potent SARS-CoV-2 neutralizing antibodies and protection from disease in a small animal model. *Science.* 2020;369(6506):956-63.
20. Cao Y, Su B, Guo X, Sun W, Deng Y, Bao L, et al. Potent neutralizing antibodies against SARS-CoV-2 identified by high-throughput single-cell sequencing of convalescent patients' B cells. *Cell.* 2020.
21. Zost SJ, Gilchuk P, Chen RE, Case JB, Reidy JX, Trivette A, et al. Rapid isolation and profiling of a diverse panel of human monoclonal antibodies targeting the SARS-CoV-2 spike protein. *Nat Med.* 2020;26(9):1422-7.
22. Lynch RJ, Silva IA, Chen BJ, Punch JD, Cascalho M, and Platt JL. Cryptic B Cell Response to Renal Transplantation. *Am J Transplant.* 2013.
23. Hussain A, Hasan A, Nejadi Babadaei MM, Bloukh SH, Chowdhury MEH, Sharifi M, et al. Targeting SARS-CoV2 Spike Protein Receptor Binding Domain by Therapeutic Antibodies. *Biomed Pharmacother.* 2020;130:110559.
24. Meng W, Zhang B, Schwartz GW, Rosenfeld AM, Ren D, Thome JJC, et al. An atlas of B-cell clonal distribution in the human body. *Nat Biotechnol.* 2017;35(9):879-84.
25. Hershberg U, and Luning Prak ET. The analysis of clonal expansions in normal and autoimmune B cell repertoires. *Philos Trans R Soc Lond B Biol Sci.* 2015;370(1676).
26. Yuan M, Liu H, Wu NC, Lee CD, Zhu X, Zhao F, et al. Structural basis of a shared antibody response to SARS-CoV-2. *Science.* 2020;369(6507):1119-23.
27. Smith K, Garman L, Wrammert J, Zheng NY, Capra JD, Ahmed R, et al. Rapid generation of fully human monoclonal antibodies specific to a vaccinating antigen. *Nat Protoc.* 2009;4(3):372-84.
28. Tiller T, Meffre E, Yurasov S, Tsuiji M, Nussenzweig MC, and Wardemann H. Efficient generation of monoclonal antibodies from single human B cells by single cell RT-PCR and expression vector cloning. *Journal of immunological methods.* 2008;329(1-2):112-24.

29. Brouwer PJM, Caniels TG, van der Straten K, Snitselaar JL, Aldon Y, Bangaru S, et al. Potent neutralizing antibodies from COVID-19 patients define multiple targets of vulnerability. *Science.* 2020;369(6504):643-50.
30. Li Q, Wu J, Nie J, Zhang L, Hao H, Liu S, et al. The Impact of Mutations in SARS-CoV-2 Spike on Viral Infectivity and Antigenicity. *Cell.* 2020;182(5):1284-94 e9.
31. Becerra-Flores M, and Cardozo T. SARS-CoV-2 viral spike G614 mutation exhibits higher case fatality rate. *Int J Clin Pract.* 2020;74(8):e13525.
32. Hou YJ, Chiba S, Halfmann P, Ehre C, Kuroda M, Dinnon KH, 3rd, et al. SARS-CoV-2 D614G variant exhibits efficient replication ex vivo and transmission in vivo. *Science.* 2020;370(6523):1464-8.
33. Weisblum Y, Schmidt F, Zhang F, DaSilva J, Poston D, Lorenzi JC, et al. Escape from neutralizing antibodies by SARS-CoV-2 spike protein variants. *Elife.* 2020;9.
34. Greaney AJ, Starr TN, Gilchuk P, Zost SJ, Binshtein E, Loes AN, et al. Complete mapping of mutations to the SARS-CoV-2 spike receptor-binding domain that escape antibody recognition. *bioRxiv.* 2020.
35. Nielsen SCA, Yang F, Hoh RA, Jackson KJL, Roeltgen K, Lee JY, et al. B cell clonal expansion and convergent antibody responses to SARS-CoV-2. *Res Sq.* 2020.
36. Davis CW, Jackson KJL, McElroy AK, Halfmann P, Huang J, Chennareddy C, et al. Longitudinal Analysis of the Human B Cell Response to Ebola Virus Infection. *Cell.* 2019;177(6):1566-82 e17.
37. Mouquet H, Scheid JF, Zoller MJ, Krogsgaard M, Ott RG, Shukair S, et al. Polyreactivity increases the apparent affinity of anti-HIV antibodies by heteroligation. *Nature.* 2010;467(7315):591-5.
38. Klein F, Diskin R, Scheid JF, Gaebler C, Mouquet H, Georgiev IS, et al. Somatic mutations of the immunoglobulin framework are generally required for broad and potent HIV-1 neutralization. *Cell.* 2013;153(1):126-38.
39. Rydyznski Moderbacher C, Ramirez SI, Dan JM, Grifoni A, Hastie KM, Weiskopf D, et al. Antigen-Specific Adaptive Immunity to SARS-CoV-2 in Acute COVID-19 and Associations with Age and Disease Severity. *Cell.* 2020.
40. Kuri-Cervantes L, Pampena MB, Meng W, Rosenfeld AM, Ittner CAG, Weisman AR, et al. Comprehensive mapping of immune perturbations associated with severe COVID-19. *Sci Immunol.* 2020;5(49).
41. Rosenfeld AM, Meng W, Chen DY, Zhang B, Granot T, Farber DL, et al. Computational Evaluation of B-Cell Clone Sizes in Bulk Populations. *Front Immunol.* 2018;9:1472.
42. Ye J, Ma N, Madden TL, and Ostell JM. IgBLAST: an immunoglobulin variable domain sequence analysis tool. *Nucleic Acids Res.* 2013;41(Web Server issue):W34-40.
43. Giudicelli V, Chaume D, and Lefranc MP. IMGT/GENE-DB: a comprehensive database for human and mouse immunoglobulin and T cell receptor genes. *Nucleic Acids Res.* 2005;33(Database issue):D256-61.
44. Rosenfeld AM, Meng W, Luning Prak ET, and Hershberg U. ImmuneDB, a Novel Tool for the Analysis, Storage, and Dissemination of Immune Repertoire Sequencing Data. *Front Immunol.* 2018;9:2107.
45. Briney B, Le K, Zhu J, and Burton DR. Clonify: unseeded antibody lineage assignment from next-generation sequencing data. *Sci Rep.* 2016;6:23901.

Figures and Figure Legends:

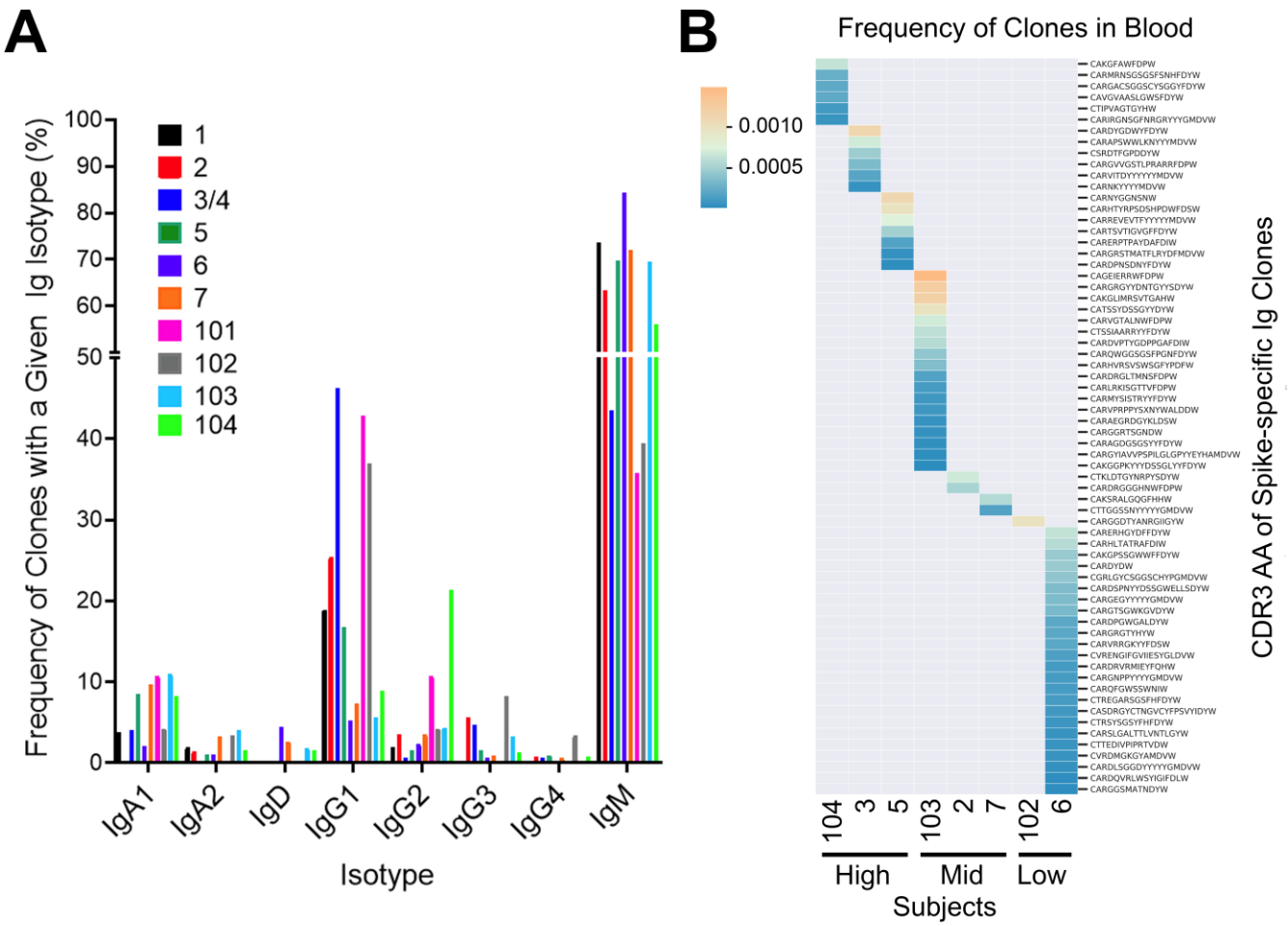

Figure 1. Properties of Spike-specific Ig sequences. Immune repertoire profiling data were generated by single cell sequencing using the 10x platform on B cells that were panned for binding to the SARS-CoV-2 spike protein (as detailed in Methods). Additional data on antibody heavy chain gene rearrangements were generated on bulk PBMC gDNA (see Methods). **(A)** Frequency of spike-specific single cell sequenced clones separated by immunoglobulin isotype. Each color indicates a subject and the height of each bar represents the frequency of spike-specific clones expressing the given isotype in that subject. **(B)** String plot of spike-binding clones that were also found in the bulk blood libraries. Each row represents a clone, each column a subject, and the intensity of each cell shows the copy number fraction of the associated spike-specific clone in the blood.

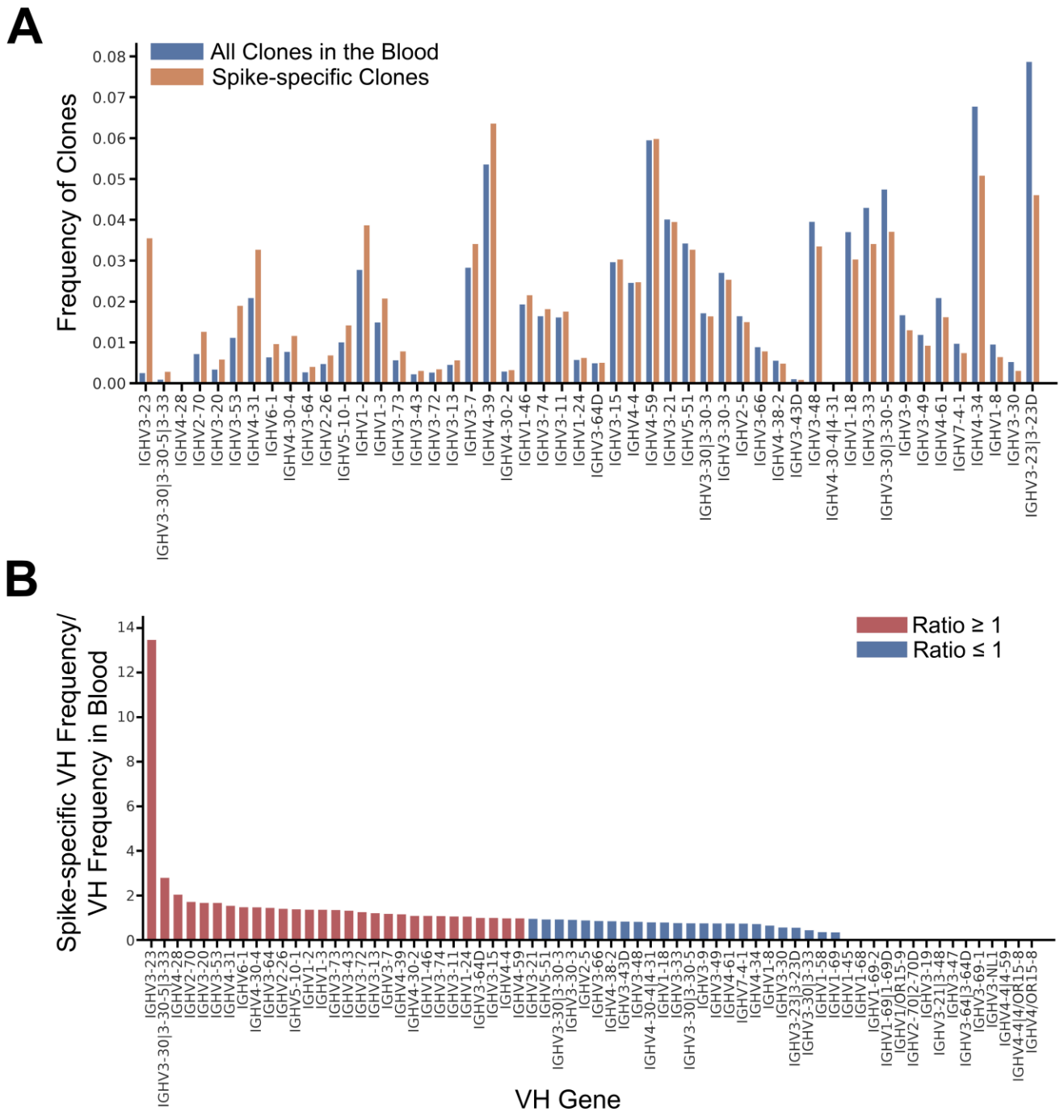

Figure 2. Comparison of the Spike-specific VH repertoire and the VH repertoire in the blood. IgH sequences were obtained from non-panned blood B cells by NGS and from spike-panned B cells as explained in the legend of Figure 1. **(A)** Number of clones utilizing the top 50 most frequent VH genes in spike-specific clones and in all clones found in the blood. Each column indicates a VH-gene, blue bars indicate the frequency of the given VH (by clone) in the blood, and the orange bar the frequency among spike-specific clones. **(B)** Fold change of VH gene frequencies in spike-enriched Ig clones as compared to VH gene frequencies in the blood. The height of each bar indicates the ratio of VH gene usage of spike-specific clones to that of other clones in the blood with the same VH. Red indicates a higher frequency in spike-binding clones and blue indicates lower frequency in spike-binding blood clones.

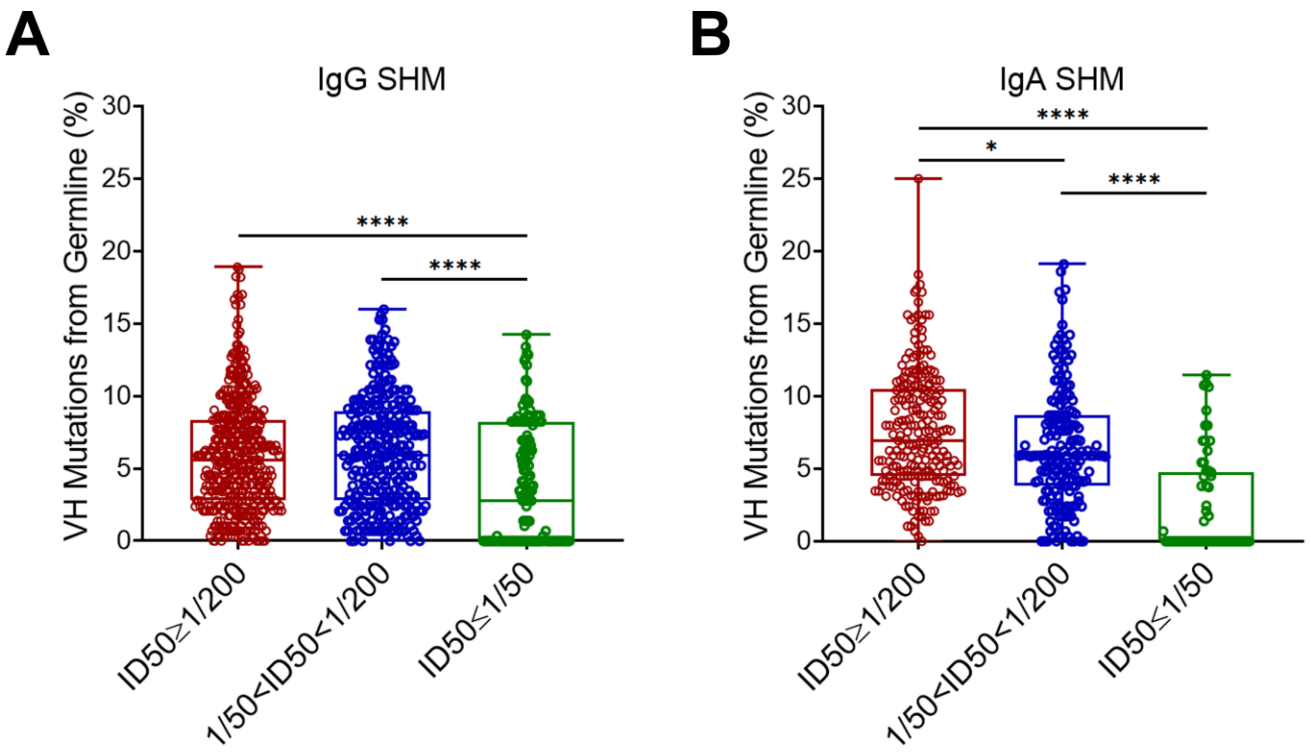

Figure 3. Somatic mutation of spike-specific VH genes according to the subjects' level of virus neutralizing antibodies in plasma. (A and B) Graphs indicate Mean±SEM of the frequency of mutated IgG (A), or IgA (B), VH sequences in relation to germline in subjects grouped by the level of virus neutralizing antibodies; low neutralizing (ID50≤1/50), mid neutralizing (1/50<ID50<1/200), high neutralizing (ID50>1/200). Analysis was by two tailed Mann/Whitney test function of Prism 9. Data represent mutations in the variable exons of all single cell IgG or IgA spike panned B cell clones.

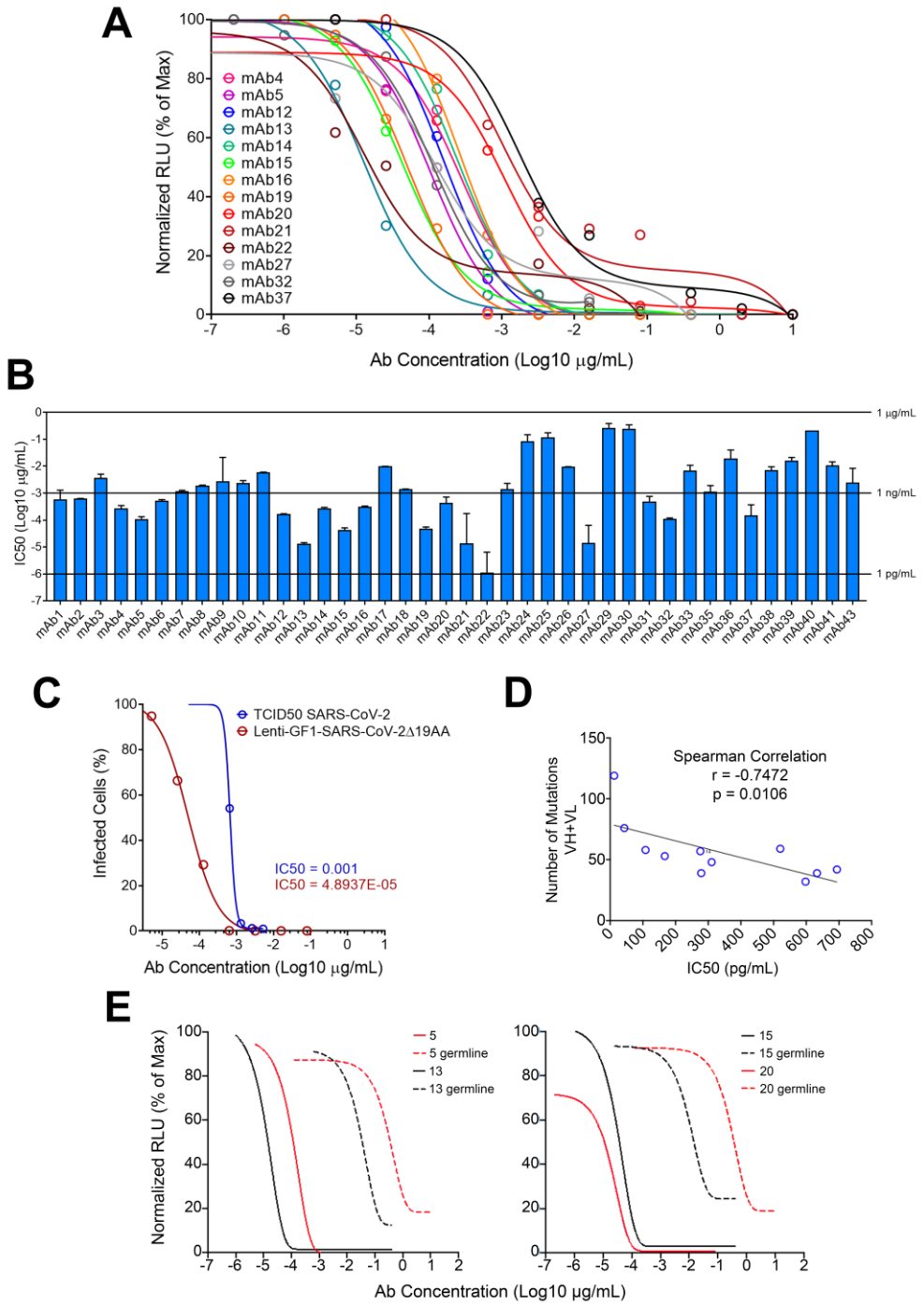

Figure 4. Neutralization of virus pseudotyped with SARS-CoV-2 Wuhan-Hu-1 spikes by human monoclonal antibodies. Highly mutated monoclonal antibodies were cloned and expressed on 293T/17 cells. The supernatants were collected and the amount of IgG was measured by ELISA. Serially diluted antibodies were incubated with viruses pseudotyped with the reference (Wuhan-Hu-1) or mutant spikes and infection of 293T-ACE2 cells was assessed by luminescence. The antibody concentration that inhibits 50% of infection (IC50) was calculated for each sample. **(A)** The neutralization curves are depicted for 40 out of 43 mAbs isolated to illustrate the breath of neutralization potency. Curves were obtained from 10 serial dilutions measured in duplicate. **(B)** The IC50 for each of the isolated MAbs. Error bars represent Mean±SEM. **(C)** The neutralization curve of MAb #19 with SARS-CoV-2 live virus, Washington USA-WA1/2020 clinical isolate and SARS-CoV-2 Wuhan-Hu-1 spike pseudotyped virus. Results were obtained from 8 serial dilutions. **(D)** Shown is the linear correlation of IC50 and number of mutations in the VH and VL genes for the 11 most potent mAbs. Analysis was by the simple linear regression followed by Spearman r test functions of Prism 9. **(E)** Neutralization curves of viruses pseudotyped with SARS-CoV-2 Wuhan-Hu-1 spike of mAbs #5, #13, #15, and #20 mutated and in germline configuration. Neutralization data curves were analyzed by non-linear fit function of Prism 9 and the absolute IC50s calculated when possible. Data reflect typical plots from at least two independent experiments.

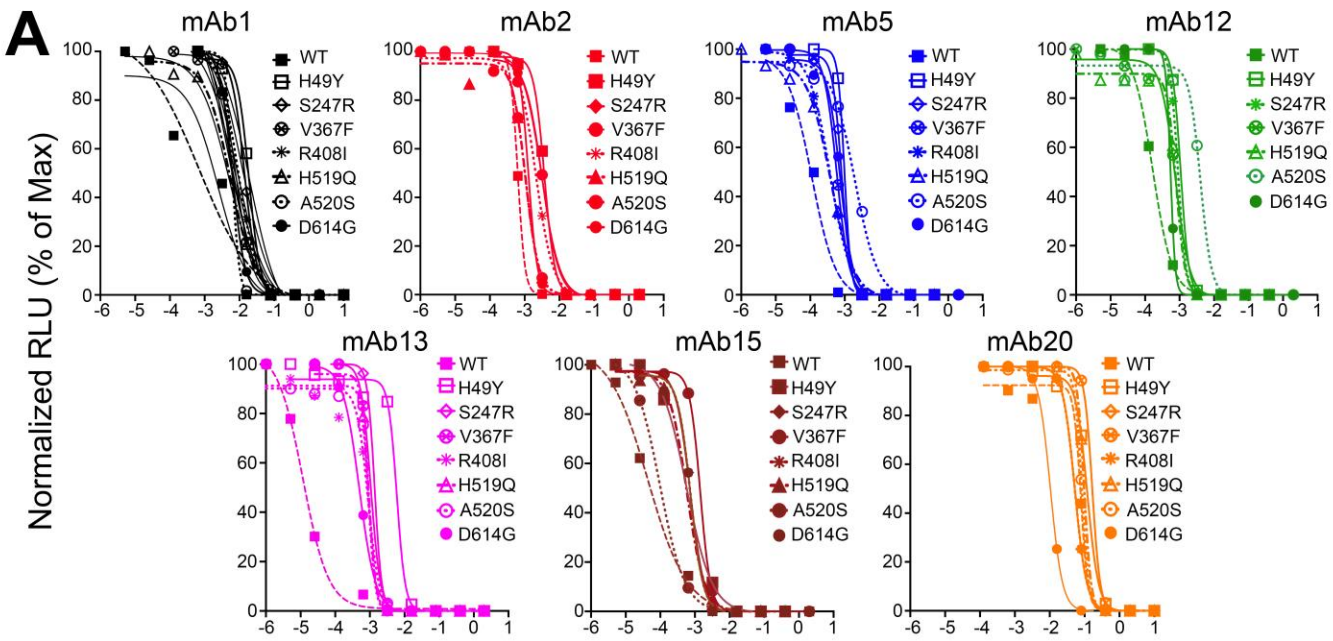

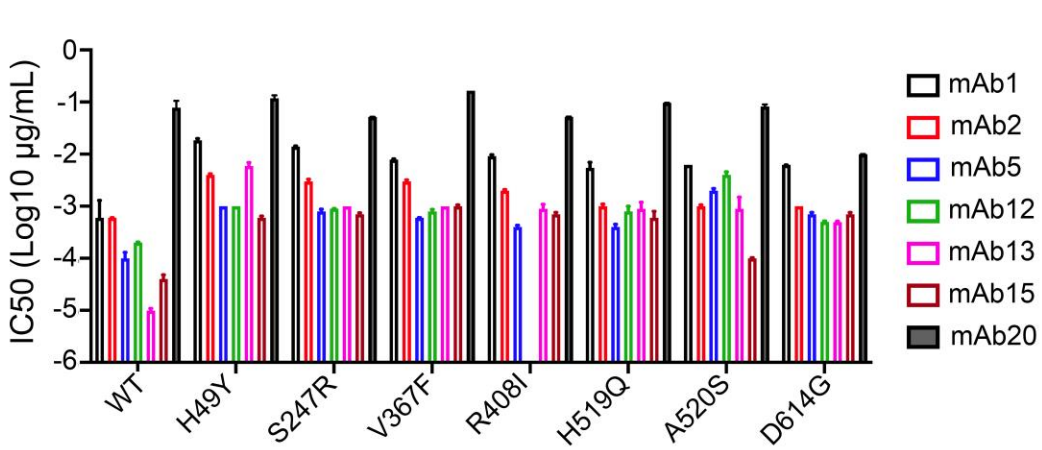

C

	S1 N-Terminal Domain					Receptor-Binding Domain		S1 C-Terminal Domain
mAb #	WT	H49Y	S247R	V367F	R408I	H519Q	A520S	D614G
1	0.000597697	0.018570605	0.014047578	0.007864395	0.009194971	0.005468077	0.00624386	0.00621747
2	0.000632813	0.003699056	0.003146481	0.002994534	0.002062502	0.001068743	0.001040948	0.00128033
5	0.000108007	0.000985643	0.000816	0.000584977	0.000373215	0.000384689	0.001923451	0.00073661
12	0.00016697	0.001081682	0.000750191	0.000750191	0.000903092	0.000798363	0.00401424	0.000547357
13	1.19703E-05	0.005993909	0.001371756	0.001063137	0.000890983	0.000920673	0.000908562	0.000494169
15	4.32153E-05	0.000565907	0.00072497	0.001414684	0.000737126	0.000580896	9.6573E-05	0.00073661
20	0.078130234	0.119280058	0.052103959	0.165540057	0.052059472	0.097018841	0.08338647	0.010412046

IC50 (Log10 µg/mL)

Figure 5. Neutralization of virus pseudotyped with SARS-CoV-2 mutant spikes by spike-specific highly mutated human monoclonal antibodies. (A) Neutralization curves of viruses pseudotyped with SARS-CoV-2 variant spikes for mAbs #1, #2, #5, #12, #13, #15, and #20. **(B)** Mean±SEM of monoclonal antibodies 50% inhibitory concentration (IC50) for SARS-CoV-2 variant spikes. **(C)** Table represents Mean±SEM of the monoclonal IgG1 antibodies IC50 for SARS-CoV-2 spikes encoding the following mutations: H49Y, S247R, V267F, R408I, V483A, H519Q, A520S and D640G. Data were analyzed by non-linear fit function of Prism 9, and the absolute IC50s calculated when possible. Data reflects a typical plot from 3 independent experiments.

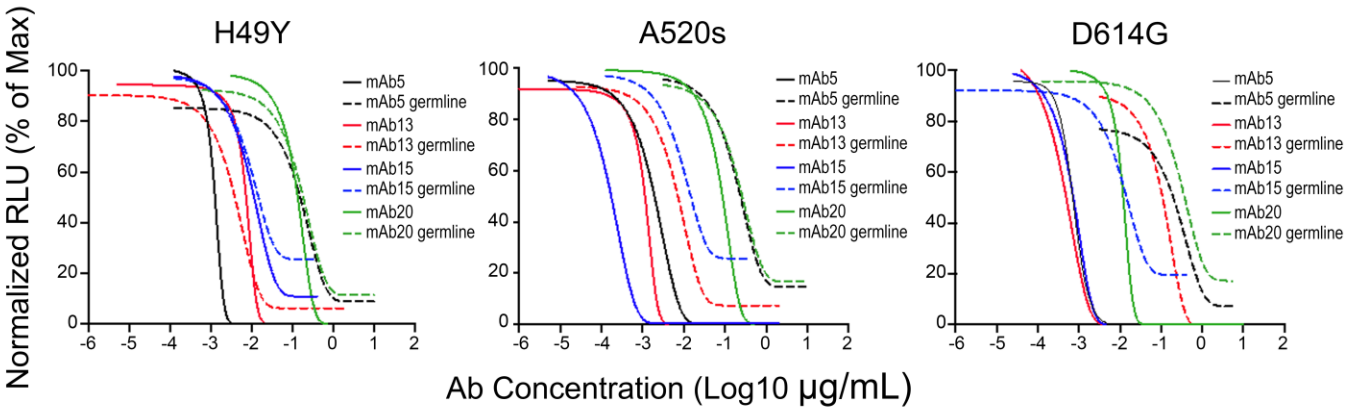

Figure 6. Neutralization of virus pseudotyped with SARS-CoV-2 mutant spikes by mature MAb and in germline configuration. The neutralization curves of viruses pseudotyped with SARS-CoV-2 H49Y, A520S and D614G spikes of mAbs #5, #13, #15, and #20 mutated and in germline configuration are shown. Data were analyzed by non-linear fit function of Prism 9, and the absolute IC50s calculated when possible. Data reflects a typical plot from 3 independent experiments.

Graphic Abstract and Caption:

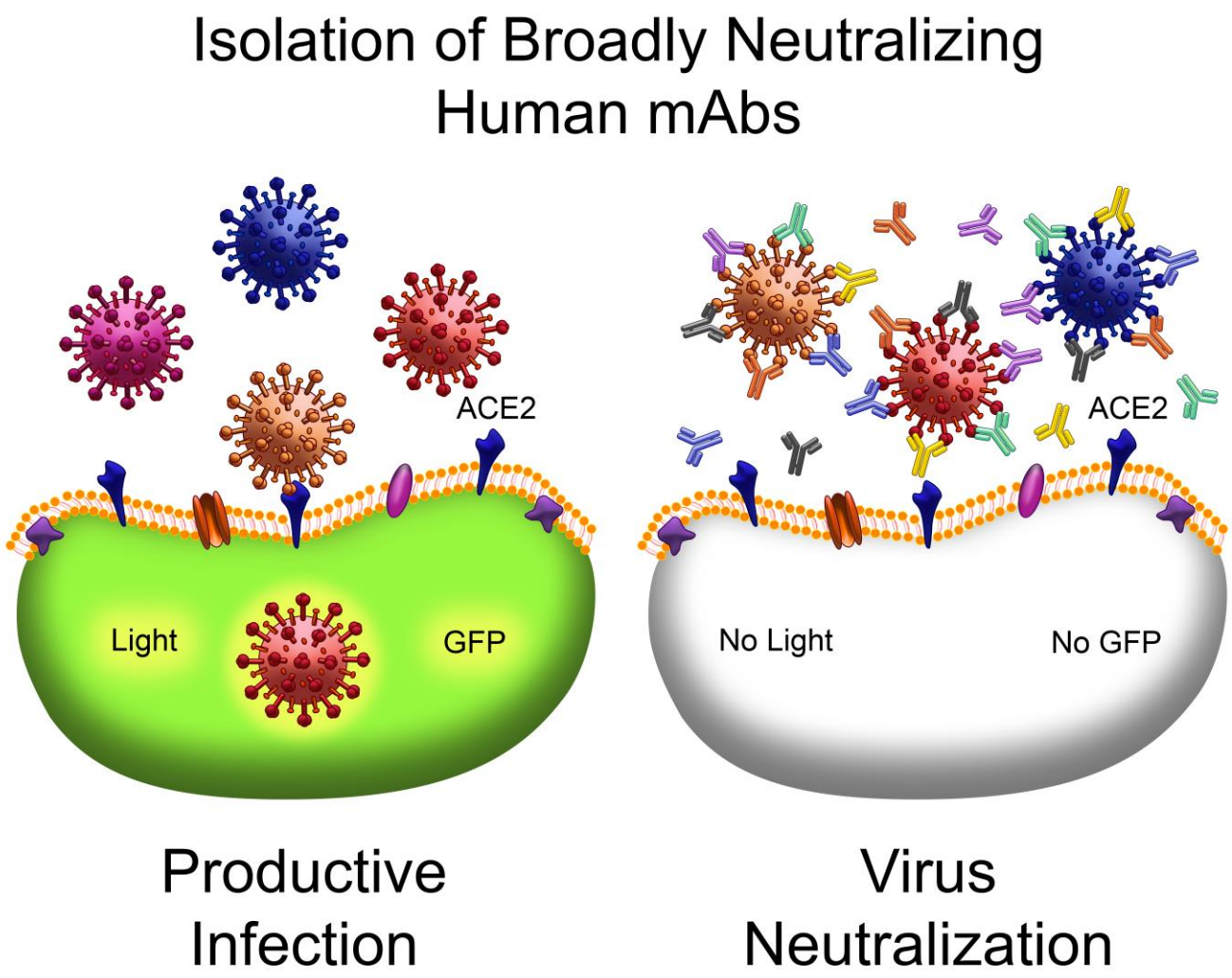

Isolation of broadly reactive human mAbs cloned from single memory spike-specific B cells. In the absence of antibodies cells expressing the virus ACE2 receptor are readily infected by diverse virus strains. Broadly reactive human mAbs neutralize virus variant strains and block infection. Virus variants and different mAbs are represented by different colors.